Title: p63 involvement in Poly(ADP-ribose) polymerase 1 signaling of Topoisomerase I-dependent DNA damage in carcinoma cells

Authors: Daniela Montariello, Annaelena Troiano, Maria Malanga, Viola Calabrò, Piera Quesada

PII: S0006-2952(13)00056-7
DOI: doi:10.1016/j.bcp.2013.01.019
Reference: BCP 11528

To appear in: *BCP*

Received date: 18-12-2012
Revised date: 21-1-2013
Accepted date: 22-1-2013

Please cite this article as: Montariello D, Troiano A, Malanga M, Calabrò V, Quesada P, p63 involvement in Poly(ADP-ribose) polymerase 1 signaling of Topoisomerase I-dependent DNA damage in carcinoma cells, *Biochemical Pharmacology* (2010), doi:10.1016/j.bcp.2013.01.019

p63 INVOLVEMENT IN POLY(ADP-RIBOSE) POLYMERASE 1 SIGNALING OF TOPOISOMERASE I-DEPENDENT DNA DAMAGE IN CARCINOMA CELLS.

Daniela Montariello, Annaelena Troiano, Maria Malanga, Viola Calabrò, Piera Quesada.

Department of Structural and Functional Biology, University of Naples "Federico II", Italy

Running Title: Effects of PARP1 and TOP I inhibitors in breast carcinoma cells

Key Words: TOP I inhibitors, PARP1 inhibitors, p53, p63, carcinoma cells.

Classification: Pharmacokinetics and Drug Metabolism

ABSTRACT

Poly(ADP-ribose)polymerase 1 (PARP-1) inhibitors are thought as breakthrough for cancer treatment in solid tumors such as breast cancer through their effects on PARP's enzymatic activity. Our previous findings showed that the hydrophilic PARP inhibitor PJ34 enhances the sensitivity of p53 proficient MCF7 breast carcinoma cells to topotecan, a DNA Topoisomerase I (TOP 1) inhibitor.

In the present study, we combine the classical TOP 1 poison camptothecin or its water-soluble derivative topotecan with PJ34 to investigate the potentiation of chemotherapeutic efficiency in MCF7 ($p53^{WT}$), MDA-MB231 ($p53^{mut}$) breast carcinoma cells and SCC022 ($p53^{null}$) squamous carcinoma cells.

We show that, following TPT/PJ34 combined treatment, MCF7 cells exhibit apoptotic death while MDA-MB231 and SCC022 cells are more resistant to these agents. Specifically, in MCF7, (i) PJ34 in combination with TPT causes a G2/M cell cycle arrest followed by massive apoptosis; (ii) PJ34 addition reverts TPT-dependent PARP-1 automodification and triggers caspase-dependent PARP-1 proteolysis; (iii) TPT, used as a single agent, stimulates p53 expression while in combination with PJ34 increases p53, TAp63α and TAp63γ protein levels with a concomitant reduction of MDM2 protein.

The identification of p63 proteins as new players involved in the cancer cell response to TPT/PJ34 is relevant for a better understanding of the PARP1-dependent signaling of DNA damage. Furthermore, our data indicate that, in response to PJ34-TPT combined chemotherapy, a functional cooperation between p53 and TAp63 proteins may occur and be essential to trigger apoptotic cell death.

1.INTRODUCTION

Poly(ADP-ribose)polymerase (PARP) inhibitors are touted as a breakthrough for cancer treatment in solid tumors such as triple negative breast cancer and ovarian cancer through their effects on PARP-1's enzymatic ADP ribosylation activity [1]; however, less characterized PARP-1 additional functions have also been reported and they can be critical for successful anticancer therapies.

PARPs are involved in the regulation of many cellular processes such as DNA repair, cell cycle progression and cell death [2]. PARP-1 and PARP-2 are constitutive factors of the DNA damage surveillance network, acting as DNA break sensor [3] and several observations indicate that poly(ADP-ribosyl)ation plays an early role in DSB signaling and repair pathways [4,5]. PARP-1 and 2 are highly activated upon binding to DNA strand interruptions and synthesize, within few seconds, large amounts of ADP-ribose polymer (PAR) on several nuclear proteins including themselves, histones, DNA-Topoisomerase 1 (TOP 1) and DNA-dependent protein kinase (DNA-PK) [6,7]. Furthermore, in response to DNA damage, PARP-1 interacts with both ATR and ATM kinases suggesting another susceptible pathway for PARP inhibitors induced apoptosis. [8].

Cell cycle checkpoint activation and growth arrest in response to DNA damage rely on the ATM/ATR kinases and their downstream targets like p53 [9-11]. p53 activates p21WAF which binds PARP-1 during base excision repair [12].

Certain PARP inhibitors including PJ34 induce a G2/M arrest when used in conjunction with methylating agents [13] cisplatin [14] and TOP I poisons such as camptothecin (CPT) or its water-soluble derivative Topotecan (TPT) [15], highlighting the existence of potentially different outcomes from PARP inhibition whose molecular mechanisms have not yet been conclusively determined.

In brief, TOP I inhibitors reversibly abolish the DNA religation activity of TOP I generating single strand breaks (SSBs) to which the protein is covalently linked. Double strand breaks (DSBs)

arise when replication forks collide with the SSBs and run off. Thus, CPT/TPT-induced DSBs are replication dependent or S phase specific and are usually repaired by the HR pathway [16,17]. According with previous findings poly(ADP-ribos)ylated PARP-1 and PARP-2 counteract CPT through non covalent but specific interaction of PAR with some TOP I sites which results in inhibition of DNA cleavage and stimulation of the religation reaction [6].

We have previously shown that PJ34 can positively or negatively modulate p53 and its target p21WAF depending of the cell genetic background or DNA damage stimulus (i.e cisplatin or TPT) [18-20]. Indeed, regulating p21WAF expression is one model whereby PARP inhibitors, following the activation of different checkpoint pathways, can cause cell cycle arrest. It has recently been reported that in breast carcinoma MCF7 cells, PJ34 causes a p21WAF-dependent mitotic arrest and that neither PARP-1 nor p53 is required for this mechanism [21]. Furthermore, in triple negative breast cancer cell lines, PJ34 synergizes with cisplatin by reducing the levels of ΔNp63α with a concurrent increase of p21WAF [22]

ΔNp63α is a member of the p53 protein family highly expressed in squamous cell carcinoma and invasive ductal breast carcinoma [23, 24]. ΔNp63α and p53 have been shown to inversely regulate target genes such as p21WAF in the context of DNA damage [22, 25]. Owing to the presence of two promoters, the p63 gene encodes two major classes of proteins: those containing a transactivating (TA) domain homologous to the one present in p53 (i.e. TAp63) and those lacking it (i.e. ΔNp63) [24]. In addition, alternate splicing at the carboxy-terminal (C-terminal) generates at least three p63 variants (α, β and γ) in each class. The TAp63γ isoform resembles most p53, whereas the α isoforms include a conserved protein-protein interaction domain named Sterile Alpha Motif (SAM). TAp63 proteins mimic p53 function including transactivating many p53 target genes and inducing apoptosis, whereas the ΔNp63α protein, has been shown to repress p53-target genes acting as an oncogene [24, 26].

On the light of all these evidences, the use of chemical inhibitors of PARP in combination with TOP I inhibitors CPT or TPT appears to be a promising approach to enhance the antitumour activity of these compounds.

Here, we have investigated the effect of PJ34 used as a single agent or in association with CPT or TPT in the DNA damage response of mammary breast cancer cells (MCF7^{p53wt} and MDA-MB231^{p53mut}) and squamous carcinoma cells (SCC022^{p53null}) showing an active involvement of p63 in the cellular response to these agents. We postulate that the sensitivity to combined treatments is mediated by sustained DNA damage/inefficient DNA repair triggering p53 and p63-mediated apoptosis.

2.MATERIALS & METHODS

Drugs, media, antibodies and chemicals

CPT and TPT was from Glaxo Smith-Kline (Verona, Italy) and PJ34 [N- (6-oxo-5,6,-dihydrophenanthridin-2-yl)-(N,N-dimethylamino) Acetamide] from Alexis Biochemicals (Vinci-Biochem, Firenze, Italy). The cocktail of protease inhibitors was from ROCHE-Diagnostic (Milano, Italy).

MCF7, MDA-MB231 and SSC022 cells were from CLS Cell Lines Service (Eppelheim, Germany) Dulbecco's modified Eagle's medium (DMEM), heat-inactivated foetal bovine serum (FBS) and Roswell Park Memorial Institute (RPMI) medium were from Invitrogen (GIBCO, Milano, Italy); penicillin, streptomycin and L-glutamine were from LONZA (Milano, Italy).

Nicotinamide adenine [adenylate-^{32}P] dinucleotide-[^{32}P]-NAD^+ (1000 Ci/mmole, 10 mCi/ml) was supplied by GE Healthcare (Milano, Italy).

PVDF (poly-vinylidene-fluoride) membrane was from MILLIPORE S.p.A. (Milano, Italy). Not-fat-milk power was from EUROCLONE (Milano, Italy). Anti-DNA TOP I (Scl-70) human antibody from Topogen (ABCAM, Cambridge, UK). Anti-PARP1 mouse monoclonal antibody (C2-10), anti-p63 (4A4), anti-p53 (DO-1), anti-p21WAF (F-5), anti-cyclin B1 (V152), anti AIF (E-1) and anti-GAPDH (6C5) mouse monoclonal antibodies and anti-actin (H-196) rabbit polyclonal antibody were from Santa-Cruz Biotechnology (DBA, Milano, Italy). Anti-γH2AX (ser139, 2577) and anti-Bax (D2E11) rabbit polyclonal antibodies were from Cell Signaling (Invitrogen, Milano, Italy). Anti-MDM2 (Ab-2) mouse monoclonal antibody was from Oncogene Research Products (Boston, USA). Anti-PAR (10H) mouse monoclonal antibody was from Alexis Biochemicals (Vinci-Biochem, Firenze, Italy). Goat anti-mouse and goat anti-rabbit IgG HRP-conjugated antibodies were from Sigma-Aldrich (Milano, Italy).

All other chemicals analytical grade were of the highest quality commercially available.

2.1 Cell cultures

Breast cancer-derived MCF7^{p53wt} and MDA-MB231^{p53mut} cells were maintained in Dulbecco's modified Eagle's medium (DMEM) containing 10% (v/v) heat-inactivated foetal bovine serum (FBS), while squamous SCC022$^{p53\ null}$ carcinoma cells were maintained in Roswell Park Memorial Institute (RPMI) medium containing 10% (v/v) FBS, 100 U/ml penicillin, 100 g/ml streptomycin, 5 mM L-glutamine and incubated at 37°C in a humidified atmosphere, *plus* 5% CO_2.

2.2 Cell Treatments

Cells were seeded at 1×10^6 cells in 10 ml and 24 h after seeding, treated with 1μM CPT (stock solution 1 mM DMSO) or 5 μM TPT ,10 x concentration inhibiting cellular growth by 50% (IC_{50}) [27]. 10 μM or 20 μM PJ34 alone and in combination, for 48 hrs in fresh medium. Culture medium was removed and, after PBS wash, cells were recovered $6x10^6$ cells/ml in 50 mM Tris–HCl pH 7.5, 150 mM NaCl, 5 mM EDTA, 1% NP40 (Lysis Buffer) plus 2 mM PMSF and 1:25 dilution of protease inhibitors cocktail solution. After 40 min of incubation on ice, cellular suspensions were scraped and centrifuged at 16000 x g for 20 min at 4°C.

Cell growth inhibition was assessed by cell counting at different time points (0-24 48 hrs) or by the 3-[4,5-dimethylthiazol-2-yl]-2,5-diphenyltetrazolium bromide (MTT) assay using $1x10^4$ 48hrs treated cells. The experiments were performed in triplicate.

2.3 Isolation of nuclear and post-nuclear fractions

To isolate sub-cellular fractions, $3x10^6$ cells were suspended in 200 μl of 30 mM Tris–HCl pH 7.5 buffer, containing, 1.5 mM $MgCl_2$, 10 mM KCl, 1% (v/v) Triton X-100, 20% glycerol, 2 mM PMSF and 1:25 dilution of protease inhibitors cocktail solution. After 30 min of incubation on ice,

cellular suspensions were centrifuged at 960 x g for 90 sec at 4°C and the nuclear fractions recovered in the pellet. The supernatant represents the cytoplasmic fraction.

Nuclear fractions were resuspended in 50 µl of 20 mM HEPES pH 7.9 buffer, containing 20 mM KCl, 0.2 mM EDTA, 1.5 mM $MgCl_2$, 25% glycerol and the protease inhibitors cocktail solution. Protein concentration was determined using the Bradford protein assay reagent (BIO-RAD Milano, Italy) with bovine serum albumin as a standard.

2.4 Cytofluorimetric analysis

Control and treated cells were fixed in 70% ethanol and stored at -20°C until analysis. After a washing in PBS w/o Ca^{++}/Mg^{++}, cells were stained in 2 ml of propidium iodide (PI) staining solution [50 µg/ml of PI, 1 mg/ml of RNAse A in PBS w/o Ca^{++}/Mg^{++}, pH 7.4] overnight at 4°C and DNA flow cytometry was performed in duplicate by a FACScan flow cytometer (Becton Dickinson Franklin Lakes, NJ USA) coupled with a CICERO work station (Cytomation). Cell cycle analysis was performed by the ModFit LT software (Verity Software House Inc. Topsham, ME USA). FL2 *area* versus FL2 *width* gating was done to exclude doublets from the G2/M region. For each sample 15,000 events were stored in list mode file.

2.5 Analysis of [^{32}P]-PAR synthesis

Following treatment with CPT/TPT +/- PJ34 of intact cell ($5x10^4$cells/plate), [^{32}P]-PAR synthesis was determined by substituting the culture medium with 1 ml of 50 mM HEPES pH 7.5 buffer, containing 28 mM KCl, 28 mM NaCl, 2 mM $MgCl_2$, 0.01% digitonin, 0.1 mM PMSF, 1:25 dilution of a cocktail of protease inhibitors, 0.125 µM NAD^+ and 5 µCi [^{32}P]-NAD^+ (1000 Ci/mmole). After incubation at 37°C for 15 mins, cells were scraped, transferred to eppendorf tubes and mixed with TCA at 20% (w:v) final concentration. After 90 min standing on ice,

samples were collected by centrifugation at 12000 rpm for 15 min, washed twice with 5% TCA and three times with ethanol. [^{32}P]-PAR incorporated in the TCA-insoluble fraction was measured by Cerenkov counting using a LS8100 liquid scintillation spectrometer (Beckman Coulter S.p.A. Milano, Italy). Finally, TCA protein pellets were resuspended in Laemmli buffer; proteins were separated by 10% SDS-PAGE and after electroblotting on PVDF membrane, [^{32}P]-PAR acceptors were visualized by autoradiographic analysis by the PhosphorImager (BIO-RAD). Immunodetection of specific proteins was accomplished on the same blots after autoradiography.

2.6 Immunological analyses

Aliquots of 10 µl of cellular proteins (approx 50-100 µg) were separated by 10% SDS-PAGE and transferred onto a PVDF membrane using an electroblotting apparatus (BIO-RAD). The membrane was subjected to immunodetection after blocking with 5% non-fat milk in TBST 1 h, with anti-PARP1 (C2-10; diluted 1:2500), anti-TOP I (Scl-70; diluted 1:1000), anti-PAR (10H; diluted 1:500) anti-p63 (4A4; diluted 1:2000) anti-p53 (DO-1; diluted 1:5000), anti-p21WAF (F-5; diluted 1:1000), anti-MDM2 (Ab-2; diluted 1:1000), anti-cyclin B1 (V152; diluted 1:1000), anti-γH2AX (2577; diluted 1:1000), anti-Bax (D2E11; diluted 1:1000), anti AIF (E1; diluted 1:2000), anti-GAPDH (6C5; diluted 1:5000), anti-actin (H-196; diluted 1:2000) overnight at room temperature.

As secondary antibodies goat-anti-mouse or goat-anti-rabbit IgG HRP-conjugate (diluted 1:5000-1:10000) in 3% (w/v) non-fat milk in TBST were used. Peroxidase activity was detected using the ECL Advance Western Blot Kit of GE Healthcare (Milano, Italy) and quantified using the Immuno-Star Chemiluminescent detection system GS710 (BIO-RAD) and the Arbitrary Densitometric Units normalised on those of the GAPDH loading control.

3. RESULTS

3.1 Effect of PJ34 on TPT/CPT-induced growth inhibition in human carcinoma cells.

The concentrations of the agents and the time points used in this study were chosen on the basis of previously published data [20, 27]. Preliminary experiments, in breast carcinoma MCF7^{p53wt} cells, showed that 1 μM CPT inhibits cell growth similarly to 5 μM TPT (**Figure 1A**). To potentiate the CPT/TPT cytostatic effect, PJ34 concentrations were used in a sub-lethal range (10-20 μM). A 48-hr of exposure, corresponding approximately to two rounds of MCF7^{p53wt} cell replication, was used according to the administration procedure during anticancer therapy. As shown in **Figure 1A,** at 24 hrs CPT/TPT treatment has a cytostatic effect, while PJ34 induces growth retardation in a dose-dependent way, whereupon cells start to recover but the rate of recovery was significantly affected by CPT/PJ34 combined treatment **(Figure 1A).**

We next investigated the impact of CPT on MDA-MB231 and SCC022 cell survival. MDA-MB231 express a mutant p53 (p53R280K) while SCC022 cells are p53 null. Cells were plated, treated with CPT for 48 hours and subjected to the MTT assay to compare viability of treated and untreated cells. As shown in **Figure 1B,** CPT significantly reduces cell viability of all cell lines tested (around 50% of control). Moreover, treatment with PJ34 alone affects MCF7 and MDA-MB231 cell viability, in a dose-dependent way, whereas SCC022 cells remain almost unaffected. Interestingly, compared with single drug treatments, combination of PJ34 with CPT results in a significant enhancement of cytotoxicity in MCF7 cells (37-33% of cell survival) while in MDA-MB231 and SCC022 cells addition of PJ34 to CPT has a lower impact on cell survival (**Figure 1B**). Similar results are observed when PJ34 is added to TPT (data not shown).

We have previously reported that TPT at concentrations higher than 1 μM promptly arrested the cells in S phase while concentrations equal or lower than 1 μM cause a G2/M arrest [20]. To gain

insight into the molecular mechanism of TPT/PJ34 interactive cytotoxicity we analysed the cell cycle distribution of MCF7 cells treated with 10 or 20 μM PJ34 alone or in combination with 1 μM TPT. As shown in **Figure 2,** after 48 hrs treatment, 1 μM TPT as well as 10 or 20 μM PJ34 induce accumulation of cells in G2/M phase and the cell cycle distribution is less affected by treatment with PJ34 (10 or 20 μM) than TPT used as single agents. Furthermore, addition of 10 or 20 μM PJ34 to 1 μM TPT causes a significant increase of G2/M cells, while S-phase cells are drastically reduced. **Figure 2 (Table)** also shows that single treatments cause an increase of cells with a sub-G1 DNA content (from 6 to 19%), probably due to induction of apoptotic cell death. Remarkably, an increase up to 55% of sub-G1 cells is observed with TPT 1 μM + PJ34 20 μM combined treatment, showing a 2x potentiation factor of PJ34 on TPT cytotoxicity.

3.2 Analysis of CPT- or TPT-dependent TOP I inactivation.

It is already known that CPT and TPT abolish the religation activity of TOP I generating an abortive complex to which the enzyme is covalently linked [16]. Therefore, we determined the efficacy of TOP I inhibitors by looking at their capacity of trapping the enzyme in the abortive complex. This was detected, by looking at the disappearance of the immunoreactive band of the TOP I soluble fraction by western blot analysis. After 48 hours of treatment, both 1 μM CPT and 5 μM TPT are able to block, almost completely, the TOP I enzyme in the abortive complex , in all cell lines tested (**Figure 3**). According to previous findings [20], PJ34 does not affect TOP I enzyme trapping when used in combination with CPT or TPT.

3.3 Analysis of PAR synthesis in carcinoma cells after treatment with TPT +/- PJ34

PJ34 efficacy as PARP inhibitor was assessed by looking at its effect on PARP-1 automodification. Proliferating MCF7 cells were exposed to the drugs and PAR synthesis was

measured *in situ* by incubation in the presence of 0.01% digitonin with 0.125 μM [^{32}P]-NAD^{+}. Samples were then analysed by SDS-PAGE followed by autoradiography. As shown in **Figure 4A**, a smear of the signal above the PARP-1 molecular weight (113 kDa) is strongly increased in TPT treated cells compared to the untreated sample **(Figure 4A, lane 4**). As previously reported [2] such a behaviour indicates automodification of PARP-1 by long and branched ADP-ribose polymers (up to 200 residues in chain) on several sites (up to 25) of the automodification domain. This process gives raise to higher molecular weight PARP-1 forms that do not enter the polyacrylamide gel matrix. The identity of the PAR modified protein was confirmed by western blotting using a PARP-1 antibody showing a mobility shift of the immunoreactive band at the top of the gel (**Figure 4B, lane 4**). According to our observation, the autoradiographic signals are absent in cells treated with the PARP-1 inhibitor alone (**Figure 4A, lanes 2 and 3**) or in combination with TPT (**Figure 4A, lanes 5 and 6**). Interestingly, TPT-PJ34 co-treatment in MCF7 cells induced apoptosis as demonstrated by the appearance of the 85 kDa fragment generated by the caspase-dependent cleavage of PARP-1 (**Figure 4B lanes 5 and 6).**

Immunoblot analysis with PARP-1 antibody was also performed in MDA-MB231 cells subjected to the same treatments. As shown in **Figure 4C**, in TPT-treated cells PARP-1 is automodified to a lower extent (**lane 4)** and there are no signs of apoptosis induction after PJ34-TPT combined treatment (**Figure 4C, lanes 5 and 6**).

Furthermore, we analysed the response of SCC022 squamous carcinoma cells to PJ34 and TPT treatment. Immunoblot with the PARP-1 specific antibody reveals that PARP-1 is modified since the unmodified 113 kDa band is strongly reduced (**Figure 4D, lanes 4 and 5**). Accordingly, immunoblot using a PAR antibody shows a smeared signal of long and branched polymers above the PARP-1 molecular weight (**Figure 4E**, **lanes 4 and 5**). PJ34 co-treatment drastically reduces TPT/CPT-induced PARP 1 automodification thus leading to the accumulation of the 113 kDa band of PARP-1. However, we did not observe PARP-1 specific cleavage, thereby suggesting that cells

were not undergoing apoptosis albeit up to 50 μM PJ34 was used (**Figure 4D, lanes 6 and 7**). All together, our results suggest that, compared to MCF7, MDA-MB231 and SCC022 cells are less sensitive to the drugs combination and do not respond immediately with apoptosis to TOP I and PARP-1 inhibitors co-treatment.

3.4 Involvement of p63 in the cell response to TPT +/- PJ34 treatment

To get insight into the molecular mechanism underlying the response of MCF7 cells to TPT +/- PJ34 treatment, we analysed the expression of p53, p63 and other cell cycle markers such as p21WAF, MDM2 and cyclin B1. In MCF7 cells we found that PJ34 addition to TPT strongly enhances the TPT-dependent stimulation of p53 expression. Remarkably, the p53 negative regulator MDM2 was down-regulated only upon combined treatment (**Figure 5A**). Furthermore, using the 4A4 monoclonal antibody which recognizes all p63 isoforms, we only detected bands corresponding to the pro-apoptotic TAp63 α and γ isoforms; both isoforms are up-regulated by TPT-PJ34 co-treatments (**Figure 5A**). Quantitation of proteins by densitometric scanning, reveals a 19-20 fold increase of the expression level for both p53 and p63 proteins after TPT-PJ34 20 μM treatment (**Figure 5B**). The increase of p21WAF expression level was concomitant to a decrease of cyclin B1 thereby supporting the G2/M cell cycle arrest observed by cytofluorimetric analyses.

We also performed immunoblot analysis of MCF7 nuclear and cytoplasmic fractions. **Figure 6A** shows that following TPT +/- PJ34 treatment both p53 and TAp63γ accumulate in the nuclear compartment. Nuclear γH2AX expression and PARP-1 specific cleavage were monitored as markers of dsDNA damage and caspase-dependent apoptosis, respectively (**Figure 6A, upper panel**). Furthermore, the expression level of the pro-apoptotic BAX protein, whose gene is transcriptionally activated by p53 and TAp63, increases in the cytoplasmic fraction by either TPT

alone or TPT-PJ34 combined treatment, while the level of the mitochondrial apoptosis inducing factor AIF is unaffected (**Figure 6A, lower panel**).

Finally, as shown in **Figure 6B**, in p53 null SCC022 cells, the ΔNp63α anti-apoptotic isoform is dramatically down-regulated by CPT/TPT treatment with or without PJ34. Cyclin B1 appears to be concomitantly reduced suggesting a G2/M cell cycle arrest. Importantly, using the 4A4 antibody, we were unable to detect p63 isoforms other than ΔNp63α both in untreated and TPT+/-PJ34 treated SCC022 cells (data not shown). It has previously been demonstrated that ΔNp63α is required for the survival of SCC cells [27]. Interestingly, as shown in **Figure 4D**, CPT/TPT +/-PJ34 treatments was not sufficient to induce apoptosis in these cells thereby suggesting the existence of an alternative anti-apoptotic pathway able to overcome ΔNp63α depletion. In MDA-MB231 cells, no p63 immunoreactive bands were seen in all experimental conditions (data not shown) thereby excluding a possible role for p63 in TPT+/-PJ34-induced cytotoxycity in this cellular context.

4. DISCUSSION

The efficacy of PARP inhibitors as chemosensitizers has led to the development of a multitude of such molecules with different bioavailability and pharmacokinetic properties that are currently under investigation in clinical trials [1]. However, a clear understanding of how PARP inhibitors potentiate the activity of antineoplastic agents is still lacking.

The hydrophilic PARP inhibitor PJ34 has already been reported to synergize with cisplatin- and TPT-dependent apoptotic induction in triple-negative breast cancer and human carcinoma cells expressing wild type p53 [19 - 22]. We have already shown that PJ34, at a concentration of 5 μM, inhibits PARP-1 activity without cytotoxic effects. Furthermore, in HeLa and MCF7 cells we found that TPT toxicity was higher when PAR synthesis was reduced by either PARP-1 silencing or PJ34 administration [20].

In the present study, we compared the response of $MCF7^{p53wt}$, $MDA\text{-}MB231^{p53mut}$ and $SCC022^{p53null}$ cells to treatment with higher concentration of PJ34 (up to 20 μM) in combination with 1 μM CPT or 5 μM TPT. According to the previously reported specificity of PARP inhibitors for breast cancer [1, 29], we observed a higher sensitivity to PJ34 in $MCF7^{p53wt}$ cells. In such cells we confirmed that TPT, which is known to be S-phase specific [30], causes a G2/M cell cycle arrest when used at a lower concentration (1 μM). In addition, the TPT-dependent G2/M cell cycle arrest was enhanced by TPT+PJ34 combined treatment and resulted in a remarkable increase of cells with sub-diploid DNA, confirming a synergic citotoxic effect of TOP I and PARP-1 inhibitors.

Consistent with the idea that poly(ADP-ribosyl)ation plays a role in the response to CPT/TPT-induced DNA damage we observed the disappearance of a TOP I soluble/active fraction and the PARP-1 automodification in MCF7, MB-MDA231 and SCC022 cells thereby indicating that the

response to DNA damage, induced by TOP I inhibitors, in skin squamous carcinoma cells is similar to that observed in breast carcinoma cells [31].

On the other hand, we found that prevention of PARP-1 automodification by PJ34 induces PARP-1 proteolysis only in MCF7^{p53wt} implying that apoptosis induced by inhibition of PAR synthesis requires the p53 wild type activity. Given the similarity between p53 and p63 it was of interest to look at the effect of TOP I + PARP-1 inhibitors on p63 protein isoforms. Interestingly,TPT+PJ34 treatment in MCF7 cells causes a remarkable increase of TAp63 α and γ protein levels. TAp63γ, in particular, was reported to be a potent apoptosis inducer [32]. Both p53 and TAp63γ accumulated in the nuclear fraction where the proteins can functionally interact in the control of transcription. Consistently, TPT+PJ34 combined treatment caused a dramatic reduction of MDM2, a negative regulator of p53 transcriptional activity and protein level.

Remarkably, this is the first evidence of a PJ34-inducible pro-apoptotic response involving both p53 and p63 family members in breast carcinoma cells. Furthermore, in SCC022^{p53null} cells we show that CPT/TPT single or combined treatments suppressed the endogenously expressed ΔNp63α anti-apoptotic isoform together with Cyclin B1. It has previously been demonstrated that ΔNp63α is required for the survival of SCC cells by virtue of its ability to suppress p73-dependent apoptosis [28]. However, CPT/TPT +/- PJ34 treatments is not sufficient to induce apoptosis in these cells thereby suggesting either the presence of a non-functional p73 or the existence of an alternative anti-apoptotic pathway able to overcome ΔNp63α depletion. Similarly, it has been reported that in MDA-MB468 cells expressing high level of ΔNp63α, PJ34 reduced ΔNp63α level, with a concomitant increase of p73. However, in that manuscript, apoptosis induction was not evaluated. [22].

Therefore, it can be postulated that carcinoma cells, depending on their genetic background (p53/p63 null versus p53/p63 proficient), can trigger a p53-dependent pathway to induce cell cycle

arrest and apoptosis, as a results of concomitant inhibition of PARP-1 and TOP I. To this respect, the particular p63 isoform expressed may sustain (TAp63α and γ) or inhibit (ΔNp63α) the execution of the apoptotic program.

Recently, it has been shown that PARP activity is required for TOP I poisoning-mediated replication fork slowing [33] and reversal [34]. In fact, PARP-1 is able to slow replication fork progression in response to CPT-dependent HR DNA repair. Furthermore, these data identify fork reversal as a means to prevent chromosome breakage upon exogenous replication stress and implicate still undefined proteins involved in fork reversal or restart as factors modulating the cytotoxicity of replication stress–inducing chemotherapeutics.

We have identified p63 as a new player of the PARP1-dependent signalling of DNA damage. Interestingly, in the p63 DNA binding domain, both the PAR binding motif and the glutamic acid residues showed to act as covalent PAR acceptor sites are conserved [35, 36]. Our findings contribute to the understanding of the molecular events triggered by TOP I and PARP-1 inhibitor-dependent genomic damage and provide a rationale for the development of new approaches to sensitize cancer cells to chemotherapy.

ACKNOWLEDGEMENTS:

This work is dedicated to the memory of Dr Maria Malanga who died November 2011, her good spirit, her ideas, her friendship and her energy are greatly missed by all her colleagues. We acknowledge Dr. Daria Maria Monti and Dr. Angela Arciello for their help with cell cultures.

REFERENCES

[1].Rouleau M, Patel A, Hendzel MJ, Kaufmann SH and Poirier GG. 2010. PARP inhibition: PARP1 and beyond. Nat.Rev.Cancer 10:293-301.

[2]. Burkle A. Poly(ADP-ribosyl)ation. LANDES Bioscience; 2005.

[3].Malanga M, Althaus FR. 2005. The role of poly(ADP-ribose) in the DNA damage signaling network. Biochem Cell Biol 83(3):354–64.

[4]. Schreiber V, Dantzer F, Ame JC, de Murcia G. 2006. Poly(ADPribose): novel function for an old molecule. Nat Rev Mol Cell Biol 7:517-28.

[5] Sugimura, K, Takebayashi, S, Taguchi, H, Takeda S, Okumura K. 2008 .PARP1 ensures regulation of replication fork progression by homologous recombination on damaged DNA. J Cell Biol 183:1203–12.

[6] Malanga M, Althaus FR. 2004. Poly(ADP-ribose) reactivates stalled DNA topoisomerase I and induces DNA strand break resealing. J Biol Chem 279(7):5244-8.

[7] Mitchell J, Smith GC, Curtin NJ. 2009. Poly(ADP-Ribose) polymerase-1 and DNA-dependent protein kinase have equivalent roles in double strand break repair following ionizing radiation. Int J Radiat Oncol Biol Phys 75(5):1520-7.

[8] Haince JF, Kozlov S, Dawson VL, Dawson TM, Hendzel MJ, Lavin MF, Poirier GG. 2007. Ataxia telangiectasia mutated (ATM) signaling network is modulated by a novel poly(ADPribose)- dependent pathway in the early response to DNA-damaging agents. J Biol Chem 282:16441–16453.

[9] Yoon JH, Ahn SG, Lee BH, Jung SH, Oh SH. 2012. Role of autophagy in chemoresistance: regulation of the ATM-mediated DNA-damage signaling pathway through activation of DNA-PKcs and PARP1. Biochem Pharmacol 83(6):747-57.

[10] Nguyen D, Zajac-Kaye M, Rubinstein L, Voeller D, Tomaszewski JE, Kummar S, Chen AP, Pommier Y, Doroshow JH, Yang SX. 2011. Poly(ADP-ribose) polymerase inhibition enhances

p53-dependent and -independent DNA damage responses induced by DNA damaging agent. Cell Cycle 10(23):4074-82.

[11] Wieler S, Gagne´ JP, Vaziri H, Poirier GG, Benchimol S. 2003. Poly(ADP-ribose) Polymerase-1 is a positive regulator of the p53-mediated G1 arrest response following ionizing radiation. J Biol Chem 278:18914–21.

[12] Cazzalini O, Donà F, Savio M, Tillhon M, Maccario C, Perucca P, Stivala LA, Scovassi AI, Prosperi E. 2010. p21CDKN1A participates in base excision repair by regulating the activity of poly(ADP-ribose) polymerase. DNA Repair 9(6):627-35.

[13] Tentori L, Graziani G. 2005. Chemopotentiation by PARP inhibitors in cancer therapy. Pharmacol Res 52:25-33.

[14] Sandhu SK, Yap TA, de Bono JS. 2010. Poly(ADP-ribose) polymerase inhibitors in cancer treatment: a clinical perspective. Eur J Cancer 46(1):9-20.

[15] Smith LM, Willmore E, Austin CA, Curtin NJ. 2005. The novel poly(ADP-Ribose) polymerase inhibitor, AG14361, sensitizes cells to topoisomerase I poisons by increasing the persistence of DNA strand breaks. Clin Cancer Res 11:8449-57.

[16] Pommier Y. 2006. Topoisomerase I inhibitors: camptothecins and beyond. Nat Rev Cancer 6:789-802.

[17] Arnaudeau C, Lundin C, Helleday T. 2001. DNA double-strand breaks associated with replication forks are predominantly repaired by homologous recombination involving an exchange mechanism in mammalian cells. J Mol Biol 307:1235–45.

[18] Cimmino G, Pepe S, Laus G, Chianese M, Prece D, Penitente R, Quesada P. 2007. Poly(ADPR)polymerase-1 signaling of the DNA damage induced by DNA topoisomerase I poison in D54(p53wt) and U251(p53mut) glioblastoma cell lines. Pharmacol Res 55(1):49-56.

[19] Gambi N, Tramontano F, Quesada P. 2008 Poly(ADPR)polymerase inhibition and apoptosis induction in cDDP-treated human carcinoma cell lines. Biochem Pharmacol 75(12):2356-63.

[20] D'Onofrio G, Tramontano F, Dorio AS, Muzi A, Maselli V, Fulgione D, Graziani G, Malanga M, Quesada P. 2011. Poly(ADP-Ribose) Polymerase signaling of topoisomerase 1-dependent DNA damage in carcinoma cells. Biochem Pharmacol 81:194-202.

[21] Madison DL, Stauffer D, Lundblad JR. 2011. The PARP inhibitor PJ34 causes a PARP1-independent, p21 dependent mitotic arrest. DNA Repair (Amst) 10(10):1003-13.

[22] Hastak K, Alli E, Ford JM. 2010. Synergistic chemosensitivity of triple-negative breast cancer cell lines to PARP inhibition, gemcitabine and cisplatin. Cancer Res 70(20):7970–80.

[23] Di Costanzo A, Troiano A di Martino O, Cacace A,Natale CF,Ventre M, Netti P, Caserta S, Pollice A, La Mantia G, Calabrò V. 2012. The p63 Protein Isoform {Delta}Np63α Modulates Y-box Binding Protein 1 in Its Subcellular Distribution and Regulation of Cell Survival and Motility Genes. J Biol Chem. 287(36):30170-80.

[24] Di Costanzo A, Festa L, Roscigno G, Vivo M, Pollice A, Morasso M, La Mantia G, Calabrò V. 2011. A dominant mutation etiologic for human Tricho-Dento-Osseus syndrome impairs the ability of DLX3 to downregulate ΔNp63α. J Cell Physiol 226(8):2189-97.

[25] Schavolt, KL, and Pietenpol JA. 2007. p53 and Delta Np63 alpha differentially bind and regulate target genes involved in cell cycle arrest, DNA repair and apoptosis. Oncogene 26:6125-32.

[26] Yang A, Kaghad M, Wang Y, Gillett E, Fleming MD, Dötsch V, Andrews NC, Caput D, McKeon F. 1998. p63, a p53 homolog at 3q27-29, encodes multiple products with transactivating, death-inducing, and dominant-negative activities. Mol Cell 2(3):305-16.

[27] Devy J, Wargnier R, Pluot M, Nabiev I, Sukhanova A. 2004. Topotecan-induced alterations in the amount and stability of human DNA topoisomerase I in solid tumor cell lines. Anticancer Res. 24(3a):1745-51.

[28] Rocco JW, Leong CO, Kuperwasser N, DeYoung MP, Ellisen LW. 2006. p63 mediates survival in squamous cell carcinoma by suppression of p73-dependent apoptosis Cancer Cell 9(1):45-56

[29] Bryant HE, Schultz N, Thomas HD, Parker KM, Flower D, Lopez E et al. 2005. Specific killing of BRCA2-deficient tumours with inhibitors of poly(ADP-ribose) polymerase. Nature 434(7035):913

[30] Feeney GP, Errington RJ, Wiltshire M, Marquez N, Chappell SC, Smith PJ. 2003. Tracking the cell cycle origins for escape from topotecan action by breast cancer cells. Br J Cancer 88(8):1310-7.

[31] Davis PL, Shaiu WL, Scott GL, Iglehart JD, Hsieh TS, Marks JR. 1998. Complex response of breast epithelial cell lines to topoisomerase inhibitors. Anticancer Res J 18(4C):2919-32.

[32] Yang A, Kaghad M, Wang Y, Gillett E, Fleming MD, Dötsch V, Andrews NC, Caput D, McKeon F. 1998. p63, a p53 homolog at 3q27-29, encodes multiple products with transactivating, death-inducing, and dominant-negative activities Mol Cell. 2(3):305-16.

[33] Sugimura, K., Takebayashi, S., Taguchi, H., Takeda, S. & Okumura, K. 2008. PARP-1 ensures regulation of replication fork progression by homologous recombination on damaged DNA. J. Cell Biol. 183: 1203–1212.

[34].Chaudhuri AR, Hashimoto Y, Herradori R, Neelsen KJ, Fachinetti D, Bermejo R, Cocito A, Costanzo V, Lopes M. 2012. Topoisomerase I poisoning results in PARP-mediated replication fork reversal. Nature Structural & Molecular Biology 19 (4): 417-24.

[35] Malanga M, Pleschke JM, Kleczkowska HE, and Althaus FR. 2000. Poly(ADP-ribose) binds to specific domains of p53 and alters its DNA binding functions. J Biol Chem 275:40974-80**.**

[36] Kanai M, Hanashiro K, Kim So-H, Hanai S, Boulares HA, Miwa M, Fukasawa K. 2007. Inhibition of Crm1–p53 interaction and nuclear export of p53 by poly(ADP-ribosyl)ation. Nat Cell Biol 9(10):1175-83.

LEGENDS TO FIGURE

Figure 1 - Cell growth inhibition in MCF7, MDA-MB231 and SSC022 cells treated with CPT/TPT and PJ34 as single agents or in combination.

Cells (10^4 cells/plate) were treated 48 hrs with CPT 1 μM or TPT 5 μM and 10 or 20 μM PJ34 alone or in combination: **A**: MCF7 cell growth was measured by cell counting at different time points. Data refer to at least three experiments giving similar results. **B**: 48 hrs treated MCF7, MDA-MB231 and SSC022 cells were used for determination of cell growth inhibition by MTT assay Each plot represents the media of triplicates from three independent experiments.

Figure 2 - Cell cycle analysis of MCF7 cells subjected to TPT and PJ34 single and combined treatments.

MCF7 cells were treated 48 hrs with TPT 1 μM and 10 or 20 μM PJ34 alone or in combination. Control and treated cells ($1x10^6$) were fixed in 70% ethanol and used for flow cytometric analysis (see Materials and Methods). Determination of DNA content after PI staining is shown and cells in G1, S and G2 phase are indicated as percentage (excluded sub-G1 cells). The table reports sub-G1 cells as the percentage of the entire population of cells. Data refer to one of three experiments giving similar results.

Figure 3. Western blot analysis of TOP I soluble fraction in carcinoma cells untreated or 48 hrs treated with the indicated drugs.

Untreated and treated whole cell extracts (50-100 μg of proteins) were subjected to 10% SDS-PAGE, electroblotted on PVDF and incubated with the anti-TOP I antibody.

Immunodetection in MCF7 (**A**) MDA-MB231 (**B)** and SSC022 (**C**) cells is shown. 0.1% DMSO treated cells were analysed as CPT internal control. GAPDH was used as loading control.

Figure 4 – Analysis of TPT-dependent PARP-1 activation or PJ34-dependent PARP-1 inhibition in carcinoma cells untreated or 48 hrs treated with the indicated drugs.

Whole cell extract (50-100 μg of proteins) after 10% SDS-PAGE and electroblotting on PVDF were either analysed by autoradiography or incubated with the different antibodies..

A: Autoradiographic analysis, of whole cell protein extract from untreated and treated MCF7 cells incubated with 0.125 μM [^{32}P]-NAD^{+} (see Materials and Methods); **B**: Immunodetection of PARP-1 on the blot shown in **A**; **C**: Immunodetection of PARP-1 in whole cell protein extract from untreated and treated MDA-MB231cells; **D:** Immunodetection of PARP-1 in whole cell protein extract from untreated and treated SCC022 cells; **E**: Immunodetection of PAR on the blot shown in **D**

Figure 5 – Western blot analysis of p53, p63, p21WAF, MDM2 and cyclin B1 expression in MCF7 cells untreated or 48 hrs treated with the indicated drugs.

Whole cell extract (50-100 μg of proteins) after 10% SDS-PAGE and electroblotting on PVDF were incubated with the different antibodies.

A: Immunodetection of p53, p63, p21WAF, MDM2, cyclin B1.GAPDH was used as loading control; **B**: p53 and TAp63 α and γ band intensities were quantified by densitometric scanning. Data expressed as Arbitrary Densitometric Units (ADU) were normalized to the internal control GAPDH. Shown are the mean of three different experiments +/-S.E.

Figure 6 – Western blot analysis of protein extract from nuclear and cytoplasmic fraction of MCF7 cells and from SCC02 cells untreated or 48 hrs treated with the indicated drugs.

Whole extract (50-100 μg of proteins) after SDS-PAGE and electroblotting on PVDF were incubated with the different antibodies.

A: Immunodetection of p53, p63, PARP-1, γH2AX, BAX, AIF in nuclear (**upper panel**) and cytoplasmic (**lower panel**) fractions from MCF7 cells. Actin and GAPDH were used as loading controls, respectively; **B**: Immunodetection of p63 and cyclin B1 in SSC022 cell extract. GAPDH was used as loading control.

Figure

Figure 1

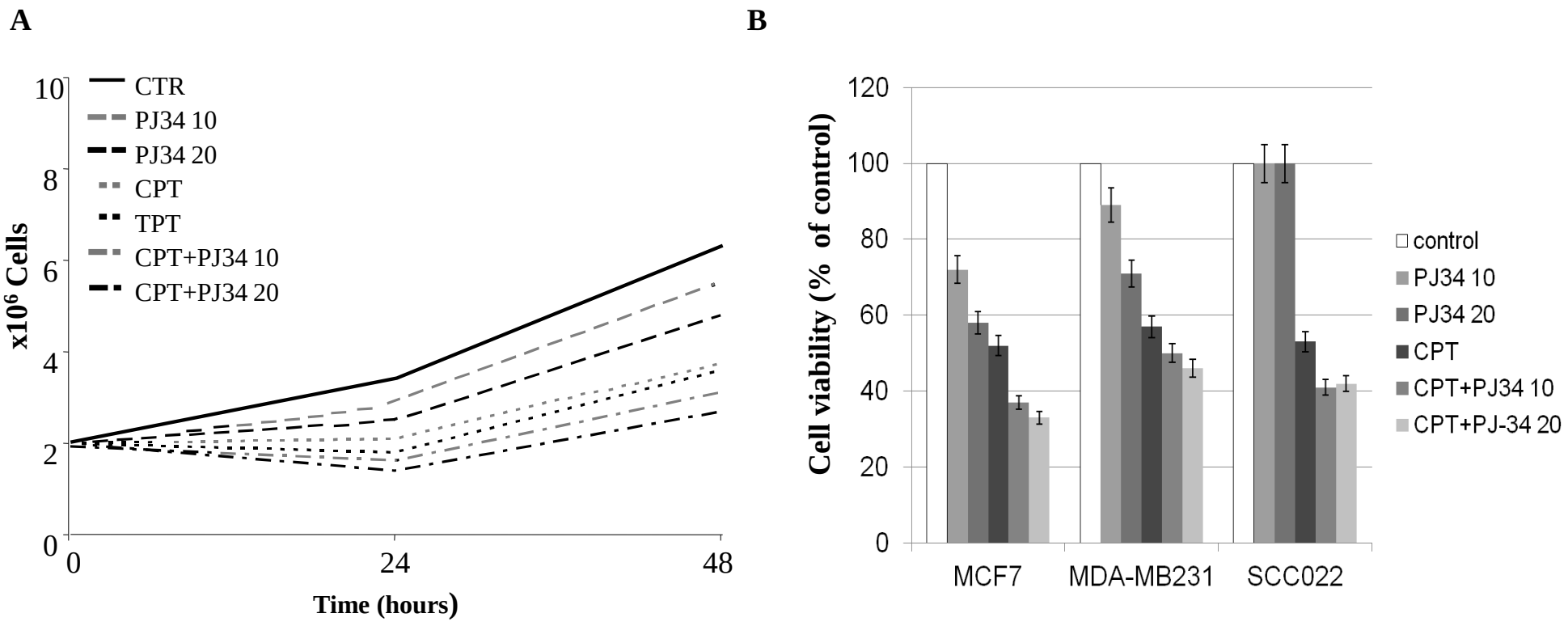

Figure 2

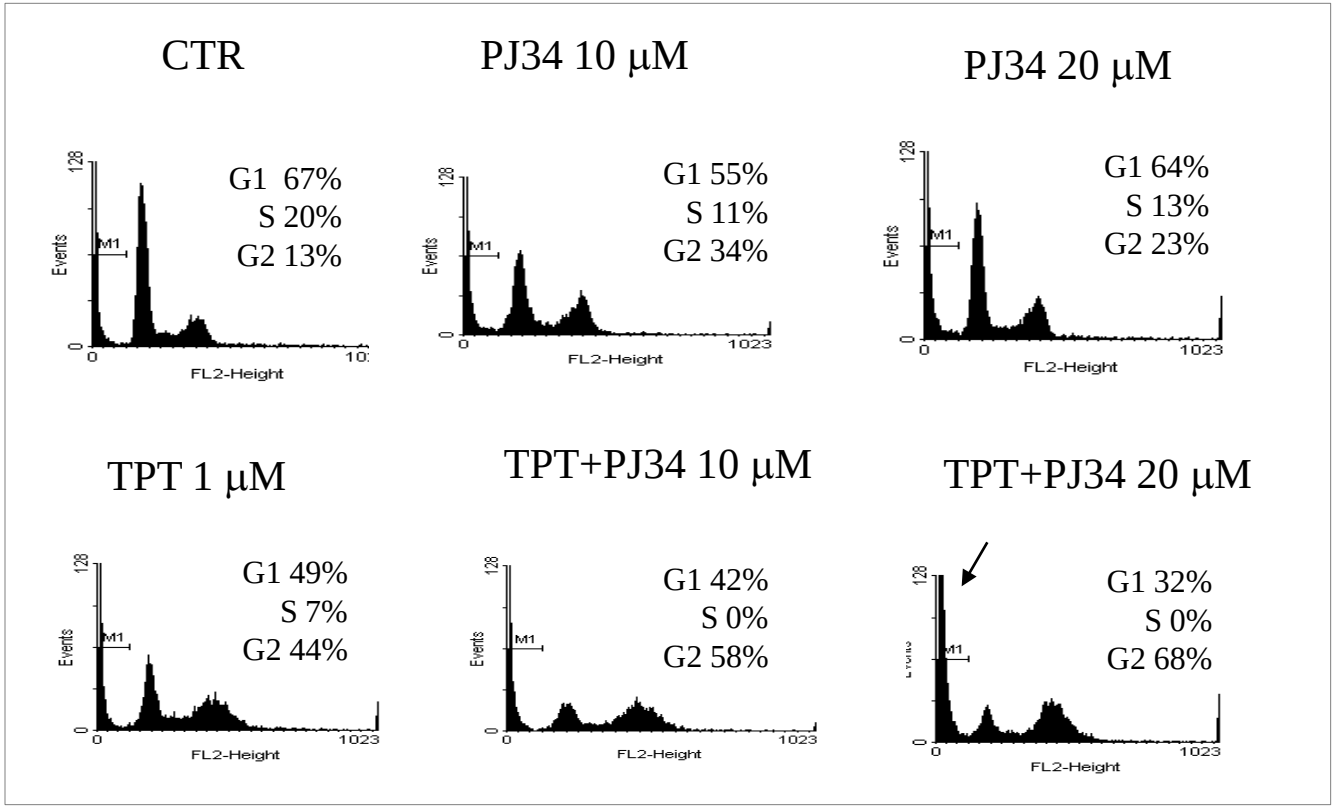

% subG1 cells

Untreated	6
TPT 1 μM	14
PJ34 10 μM	16
PJ34 20 μM	19
TPT 1 + PJ34 10μM	22
TPT 1 + PJ34 20μM	55

MCF7

Figure 3

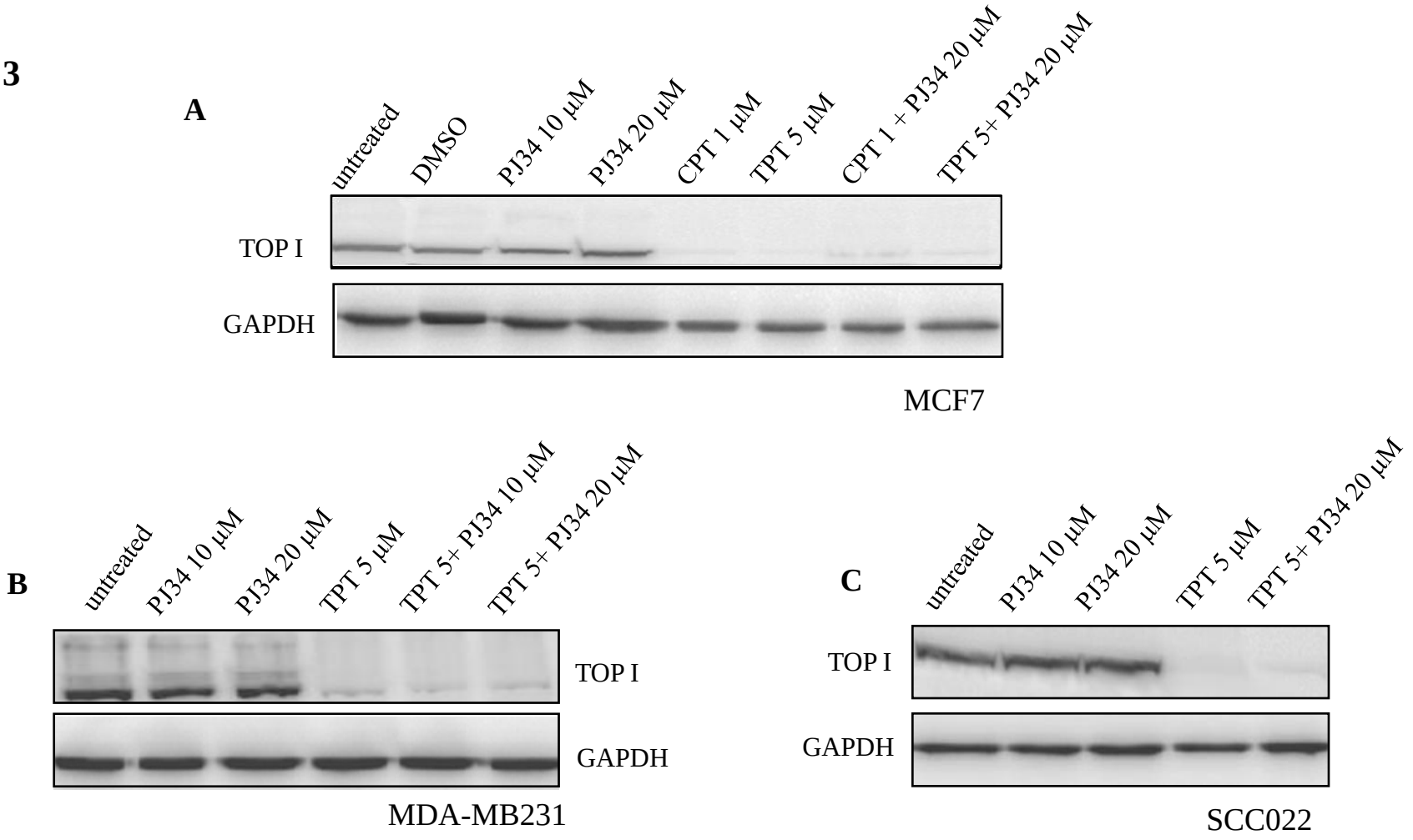
A
untreated
DMSO
PJ34 10 µM
PJ34 20 µM
CPT 1 µM
TPT 5 µM
CPT 1 + PJ34 20 µM
TPT 5+ PJ34 20 µM
TOP I
GAPDH
MCF7
B
untreated
PJ34 10 µM
PJ34 20 µM
TPT 5 µM
TPT 5+ PJ34 10 µM
TPT 5+ PJ34 20 µM
TOP I
GAPDH
MDA-MB231
C
untreated
PJ34 10 µM
PJ34 20 µM
TPT 5 µM
TPT 5+ PJ34 20 µM
TOP I
GAPDH
SCC022

Figure 4

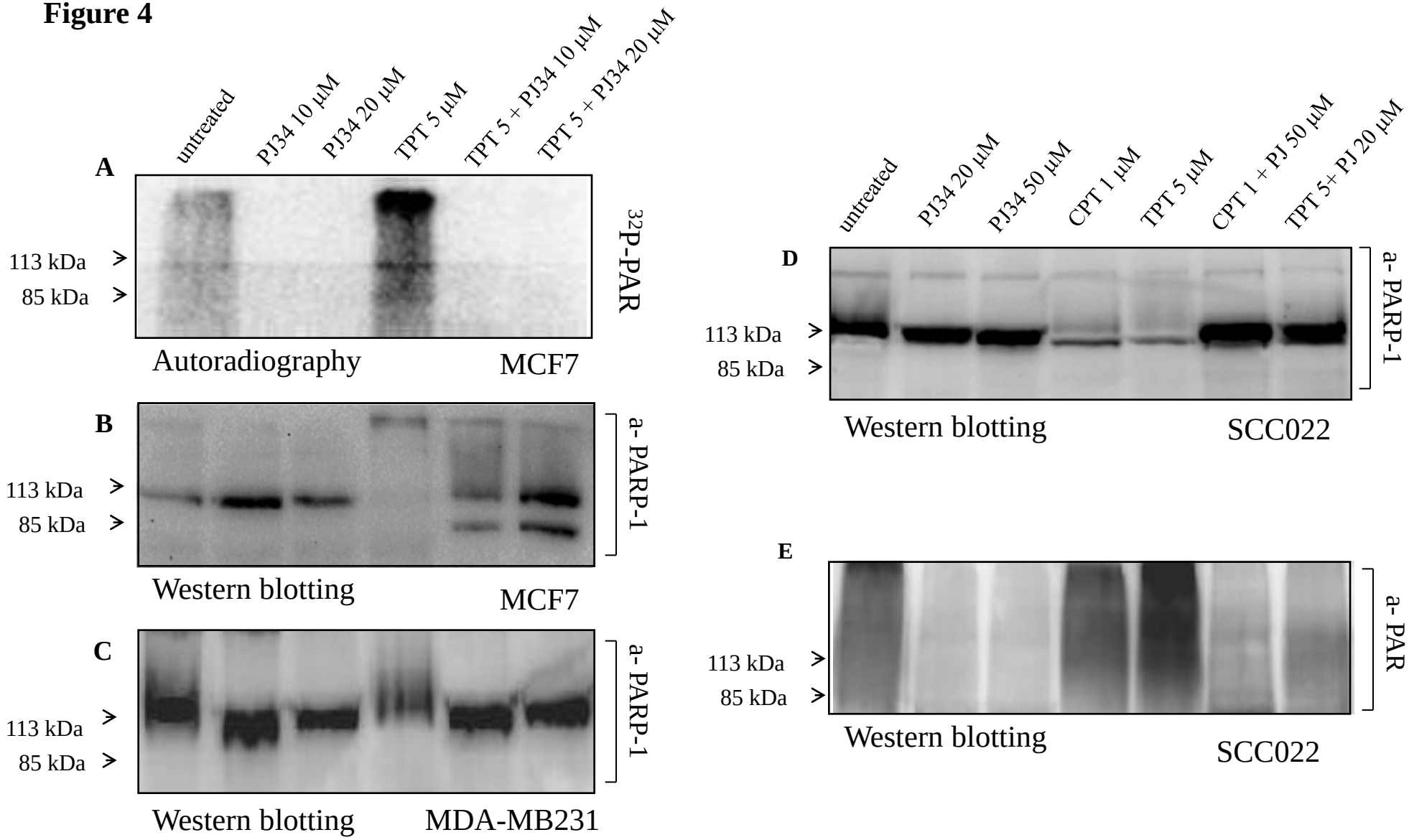
untreated
PJ34 10 μM
PJ34 20 μM
TPT 5 μM
TPT 5 + PJ34 10 μM
TPT 5 + PJ34 20 μM
A
113 kDa
85 kDa
32P-PAR
Autoradiography
MCF7
B
113 kDa
85 kDa
a- PARP-1
Western blotting
MCF7
C
113 kDa
85 kDa
a- PARP-1
Western blotting
MDA-MB231
untreated
PJ34 20 μM
PJ34 50 μM
CPT 1 μM
TPT 5 μM
CPT 1 + PJ 50 μM
TPT 5+ PJ 20 μM
D
113 kDa
85 kDa
a- PARP-1
Western blotting
SCC022
E
113 kDa
85 kDa
a- PAR
Western blotting
SCC022

Figure 5

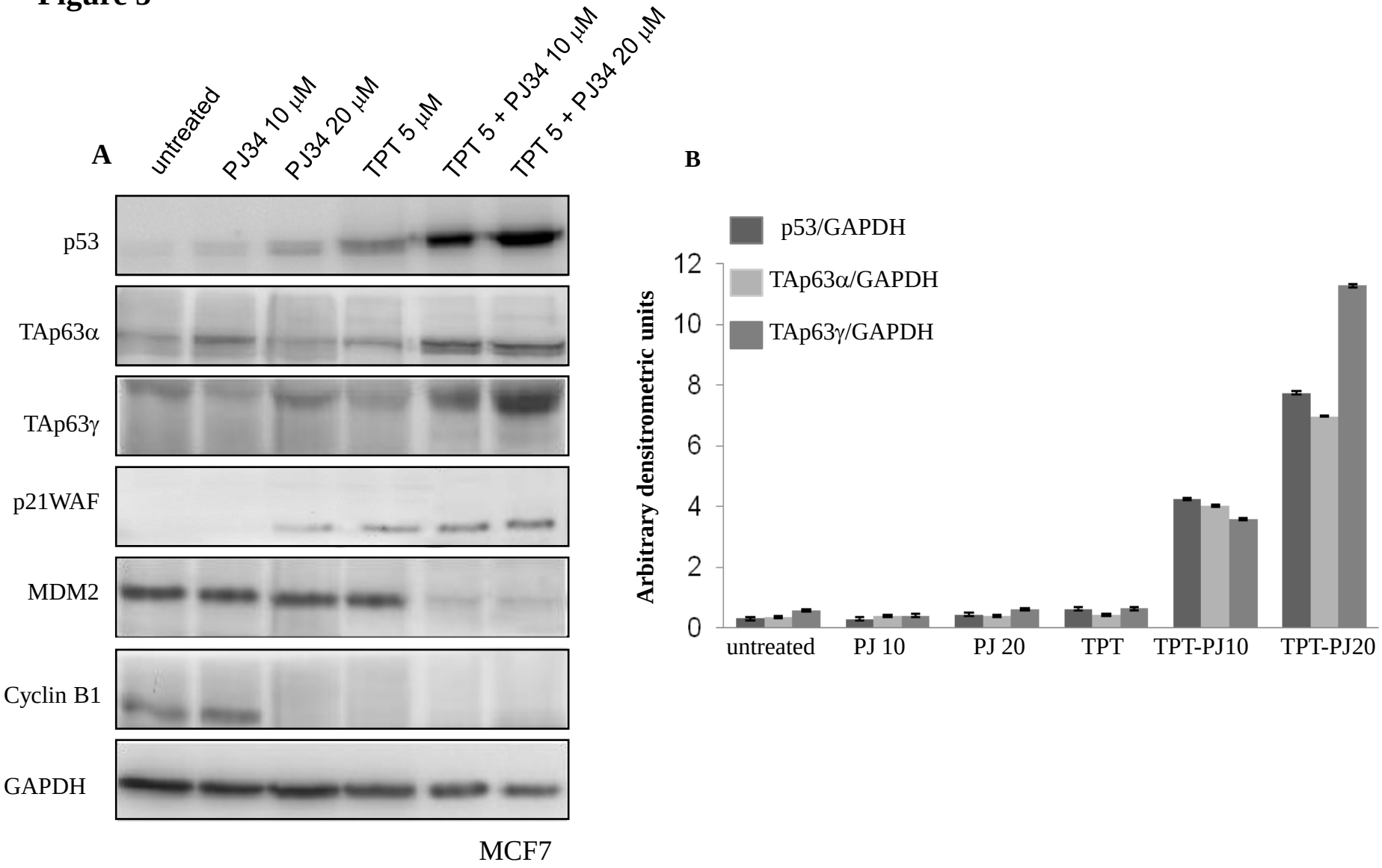
A
untreated
PJ34 10 μM
PJ34 20 μM
TPT 5 μM
TPT 5 + PJ34 10 μM
TPT 5 + PJ34 20 μM
p53
TAp63α
TAp63γ
p21WAF
MDM2
Cyclin B1
GAPDH
MCF7
B
p53/GAPDH
TAp63α/GAPDH
TAp63γ/GAPDH
Arbitrary densitrometric units
0
2
4
6
8
10
12
untreated
PJ 10
PJ 20
TPT
TPT-PJ10
TPT-PJ20

Figure 6

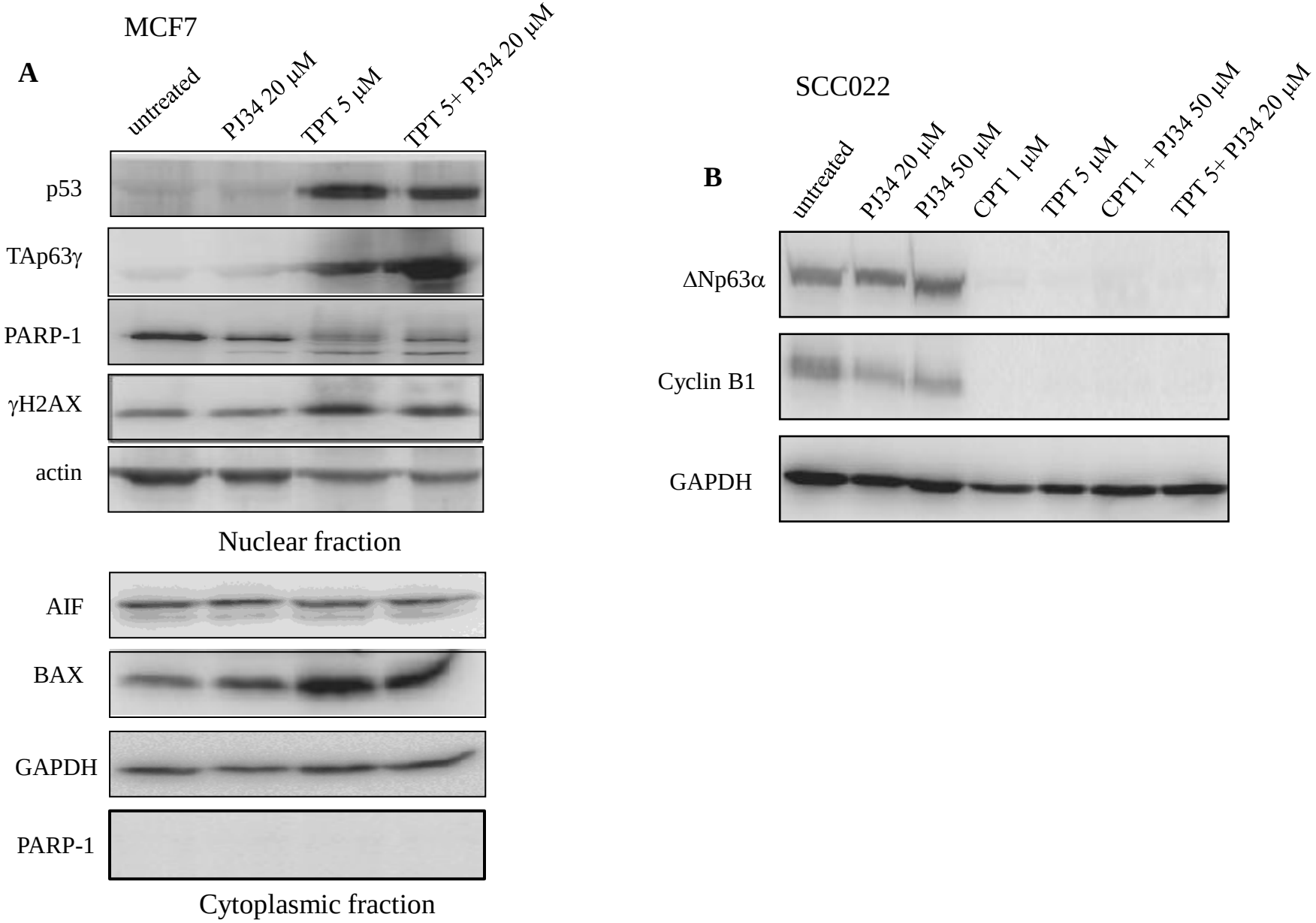
A
MCF7
untreated
PJ34 20 μM
TPT 5 μM
TPT 5+ PJ34 20 μM
p53
TAp63γ
PARP-1
γH2AX
actin
Nuclear fraction
AIF
BAX
GAPDH
PARP-1
Cytoplasmic fraction
B
SCC022
untreated
PJ34 20 μM
PJ34 50 μM
CPT 1 μM
TPT 5 μM
CPT1 + PJ34 50 μM
TPT 5+ PJ34 20 μM
ΔNp63α
Cyclin B1
GAPDH

*Graphical Abstract (for review)

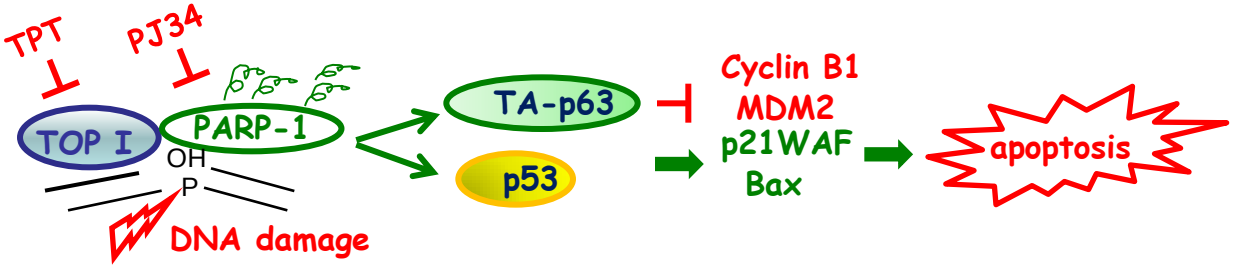

In response to combined treatment with TOP I and PARP-1 inhibitors, a functional cooperation between p53 and TAp63 proteins can take place to trigger apoptosis in carcinoma cells.